Journal of Applied Polymer Science

Thermally Induced Crystallization and Enzymatic Degradation Studies of Poly (L-Lactic Acid) Films

Nadarajah Vasanthan, Hande Gezer
Department of Chemistry, Long Island University, Brooklyn, New York 11201
Correspondence to: N. Vasanthan (E-mail: nadarajah.vasanthan@liu.edu)

ABSTRACT: Poly(L-lactic acid) (PLLA) films with different crystallinities were prepared by solvent casting and subsequently annealed at various temperatures (T_a) (80–110°C). The effects of crystallinity on enzymatic degradation of PLLA films were examined in the presence of proteinase K at 37°C by means of weight loss, DSC, FTIR spectroscopy, and optical microscopy. DSC and the absorbance ratio of 921 and 956 cm^{-1} (A_{921}/A_{956}) were used to evaluate crystallinity changes during thermally induced crystallization and enzymatic hydrolysis. The highest percentage of weight loss was observed for the film with the lowest initial crystallinity and the lowest percentage of weight loss was observed for the film with highest crystallinity. FTIR investigation of degraded films showed a band at 922 cm^{-1} and no band at 908 cm^{-1} suggested that all degraded samples form α crystals. The rate of degradation was found to depend on the initial crystallinity of PLLA film and shown that enzymatic degradation kinetics followed first-order kinetics for a given enzyme concentration. DSC crystallinity and IR absorbance ratio, A_{921}/A_{956} ratio, showed no significant changes with degradation time for annealed PLLA films whereas as-cast PLLA film showed an increase in crystallinity with degradation; this revealed that degradation takes place predominantly in the free amorphous region of annealed PLLA films without changing long range and short range order © 2012 Wiley Periodicals, Inc. J. Appl. Polym. Sci. 000: 000–000, 2012

KEYWORDS: poly(L-lactic acid); enzymatic degradation; FTIR spectroscopy; crystallinity; weight loss and kinetics of degradation

Received 5 March 2012; accepted 2 May 2012; published online 00 Month 2012
DOI: 10.1002/app.38015

INTRODUCTION

Biodegradable polymers are of growing interest in the field of drug delivery systems, surgical sutures, and tissue engineering applications. Poly(L-lactic acid) (PLLA) is one of the most promising biodegradable and biocompatible aliphatic polyesters; it is also produced from renewable resources. Optical, physical, mechanical, and barrier properties of PLLA are comparable to petroleum-based polymers.[1–6] PLLA is used for a variety of other commercial applications, such as packaging films and fibers, due to its mechanical and physical properties.[7,8] PLLA can be crystallized either by thermally induced or strain-induced crystallization.[9,10] Crystallinity and molecular orientation of PLLA are important parameters in determining the physical and mechanical properties, as well as the biological responses, of PLLA.[11–13]

Crystallization of PLLA has been carried out either by solution crystallization or melt crystallization to obtain different structures. PLLA can crystallize into three crystal forms, α, β, and γ, depending on the crystallization conditions.[14–18] The α crystal form is the most common one and is usually prepared either by melt or cold crystallization of PLLA. The β crystal form is produced during strain-induced crystallization of PLLA films at a high draw ratio and high drawing temperature or spinning fibers at a high spinning speed. de Santis and Kovacs showed that the α crystal form of PLLA from solution-spun fibers has a pseudo-orthorhombic unit cell containing two left-handed 10_3 polymeric helices that are arranged in an antiparallel fashion.[19] The unit cell dimensions of the α crystal form are $a = 1.07$ nm, $b = 0.645$ nm, and $c = 2.78$ nm. Hoogsteen et al. showed that the β form of PLLA adopts an orthorhombic unit cell containing six left-handed 3_1 polymeric helices. The unit cell dimensions of the β form are $a = 1.031$ nm, $b = 1.821$ nm, and $c = 0.900$ nm.[20,21]

The degradability of PLLA has been investigated by numerous researchers.[22–37] The effect of structural parameters on hydrolysis of PLLA in different media, such as phosphate-buffered solution (pH = 7.4), an alkaline media, acidic media, and enzymes, have also been studied extensively.[22–37] It has been demonstrated from these studies that hydrolysis of PLLA films proceeds through a surface erosion mechanism in the presence of an alkaline media or enzyme, whereas it proceeds homogenously along the film in a phosphate-buffered solution and acid

media. The hydrolytic degradation of PLLA films in an alkaline solution was studied using weight loss and high-performance liquid chromatography (HPLC) by Vasanthan and Ly.[37] It has been shown that the degradation of PLLA films increased with increasing crystallinity, which suggested that base hydrolysis occurs predominantly by a surface erosion mechanism.

Enzymatic degradation studies of melt crystallized PLLA have been studied[13,14,32–35] and shown that enzymatic hydrolysis rate decrease with increasing cystallinity. Crystallinity of degraded PLLA film measured by differential scanning calorimetry (DSC) showed an increase with degradation time. In our study, enzymatic degradation of PLLA film showed no significant change in crystallinity with degradation time and it was not in agreement with earlier work on enzymatic degradation of PLLA. The aim of this work is to revisit the enzymatic degradation of PLLA and characterize microstructural changes by FTIR spectroscopy and DSC and propose a possible mechanism for enzymatic degradation of PLLA.

EXPERIMENTAL

Materials

Poly (L-lactic acid) with a molecular weight of 300,000 was obtained from Polysciences, Inc. The enzyme proteinase K from Tritirachim album, sodium lactate 60% (w/w) solution with a density of 1.3 g/mL, and trizma hydrochloride (Tris-HCl) were purchased from Sigma-Aldrich. PLLA films were prepared using a solvent-casting method. PLLA pellets (0.2 g) were dissolved in 20 mL of dichloromethane and the solution was poured into a glass Petri dish. The solution was kept at room temperature for 16 h for evaporation of dichloromethane and a film with a thickness of 50–60 μ was obtained. The prepared films were kept in a vacuum at room temperature for further drying until constant mass. After drying, some of the PLLA films were annealed isothermally at 80, 95, and 110°C in the oven for 30 min to obtain PLLA films with different crystallinities. PLLA as-cast and annealed at 80, 95, and 110°C were labeled as PLLA25, PLLA80, PLLA95, and PLLA110, respectively.

Enzymatic Degradation

Enzymatic degradation studies of PLLA films and films annealed at various temperatures were performed using the enzyme proteinase K at 37°C. The films were cut into 1 inch × 1 inch dimensions. An enzyme solution was prepared by dissolving 1.0 mg of proteinase K enzyme in 1 mL of the e-pure water. The 0.05*M* Tris-HCl with a pH 8.5 buffer solution was prepared by adjusting the pH of 50 mL of 1.0*M* Tris-HCl solution with 1.0*M* NaOH and diluting with 1.0 L of e-pure water. Then 1.0 mL of the enzyme solution and 9.0 mL of Tris-HCl buffer were added to a 100.0 mL beaker and a PLLA film was placed in this solution. The enzymatic degradation at 37°C was followed by measuring weight loss of PLLA for predetermined degradation time intervals up to 9 days. PLLA films were removed from the beaker and washed with cold water and vacuum-dried for 24 h at 40°C to a constant weight. After 2, 4, 6, and 9 days, the enzyme solutions in the beakers were changed to keep the enzyme activity similar during the degradation process.

Weight Loss Measurements

PLLA films were taken out from the solutions after 2, 4, 6, and 9 days and washed with cold water. Films were wiped and placed in the vacuum for approximately an overnight at 40°C. The percentage of weight loss was calculated using the initial and final weight of the PLLA films using the following equation:

$$W_{\text{loss}}(\%) = 100 \times (W_{\text{before}} - W_{\text{after}})/W_{\text{before}}.$$

where W_{loss} (%) is the percentage of weight loss of the hydrolyzed PLLA film, W_{before} is the weight of the dried PLLA film before hydrolysis, and W_{after} is the weight of the dried PLLA film after hydrolysis.

DSC Analysis

Glass transition temperature, melting temperature, and enthalpy of fusion were determined using DSC. Perkin Elmer DSC 7 was used for the DSC analysis. A sample of 4–6 mg was placed into the aluminum pans and DSC scans were collected between 30 and 200°C to obtain the glass transition temperature (T_g), cold crystallization temperature (T_c), melting temperature ($T_{m,}$) and heat of fusion. The instrument was calibrated using onset and heat of fusion values of indium (T_m = 156.6°C, ΔH = 28.5 J/g). Peak analysis was carried out for all samples selecting linear baseline between 160 and 180°C. The degree of crystallinity, $\chi_{c,}$ was calculated from the heat of fusion and obtained from the DSC scans using the following equation:

$$\%\chi_c = \frac{\Delta H_m - \Delta H_c}{\Delta H_{100\%}} \times 100.$$

where ΔH_m is the enthalpy of melting, ΔH_c is the enthalpy of crystallization, and $\Delta H_{100\%}$ is the heat of fusion of 100% crystalline PLLA. Crystallinity values for PLLA were determined using the heat of fusion of 100% crystalline PLLA for all samples (93 J/g).[37]

FTIR Spectroscopy

Nicolet Magna 760 Spectrometer was used for the FTIR analysis. The spectra were collected in the mid-IR region from 4000 to 500 cm^{-1} with a resolution of 4 cm^{-1} using 64 scans to obtain adequate signal-to-noise ratio. The spectra of annealed films and the room temperature films were taken before and after degradation and the results were compared. Peak areas were obtained using Omnic software by taking the area under the peaks.

RESULTS AND DISCUSSION

Crystallization and Morphology of Solvent Cast PLLA Films

Thermal properties of PLLA films annealed at different temperatures were investigated by DSC. DSC scans of PLLA25, PLLA80, PLLA95, and PLLA110 are shown in Figure 1. Three transitions, glass transition (T_g), cold crystallization peak (T_c), and melting transition (T_m), can be seen for the as-cast PLLA film; whereas, the PLLA-80 show two transitions (T_g and T_m) and PLLA95 and PLLA110 show only T_m. The cold crystallization peak was observed at around 90°C only for PLLA-25 and disappears for PLLA80, PLLA95, and PLLA110, suggesting that

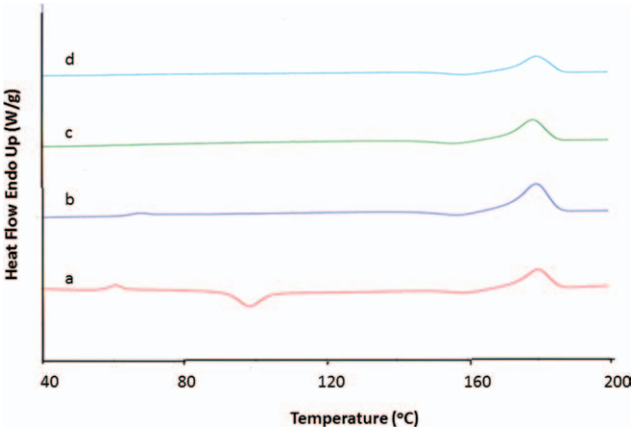

Figure 1. DSC scans of PLLA at annealing temperature (T_a) of 25, 80, 95, and 110°C. [Color figure can be viewed in the online issue, which is available at wileyonlinelibrary.com.]

all of the annealed films have a significant amount of crystallinity. A melting transition is apparent at 170°C in the DSC heating scan of PLLA25, PLLA80, PLLA95, and PLLA110, indicating that annealing does not significantly alter the lamellar thickness. Crystallinity values obtained by DSC for PLLA25, PLLA80, PLLA95, and PLLA110 are given in Table I. Each piece of data in Table I is the average of at least four determinations. Crystallinity of PLLA film appears to increase with increasing T_a.

FTIR spectra of PLLA films were studied in detail and the band assignments were reported.[37–39] It was demonstrated that IR region 1400–600 cm^{-1} is highly sensitive to structural changes. FTIR spectra in the region 1500–1250 cm^{-1} and 1000–600 cm^{-1} of annealed PLLA films are shown in Figure 2(A, B), respectively. The bands at 1385, 1360, 1304, 1293, 921, 872, 756, and 695 cm^{-1} were attributed to crystalline phase and the bands at 1368, 1300, 1267, 956, 848, 737, and 711 cm^{-1} were attributed to amorphous phase. It is well known that PLLA crystallizes into three possible crystal forms: α, β, and γ crystal forms. The most common α crystal form is obtained either by melt or solution crystallization while β crystal form is obtained during drawing at high draw ratios and temperatures. The γ form was obtained during epitaxial crystallization. Infrared band assignments were reported. The band at 921 cm^{-1} was attributed to α crystalline phase, the band at 908 cm^{-1} was attributed to β crystalline phase and the band at 956 cm^{-1}

Table I. DSC Crystallinity ($\%\chi_c$), FTIR Crystallinity ($\%\chi_c$), Absorbance Ratio of Crystalline and Amorphous Bands (A_{921}/A_{956}), Rate Constant and Half-Life ($t_{½}$) of PLLA Films Annealed at Various Temperatures

Sample	($\%\chi_c$) From DSC	A_{921}/A_{956}	($\%\chi_c$) From FTIR	%Weight loss	k (h^{-1})	$t_{½}$ (h)
PLLA25	16.0	0.116	14	40.8	0.0025	277
PLLA80	32.0	0.809	39	17.7	0.0010	693
PLLA95	34.0	0.993	45	11.2	0.0005	1386
PLLA110	37.0	1.059	47	5.4	-	-

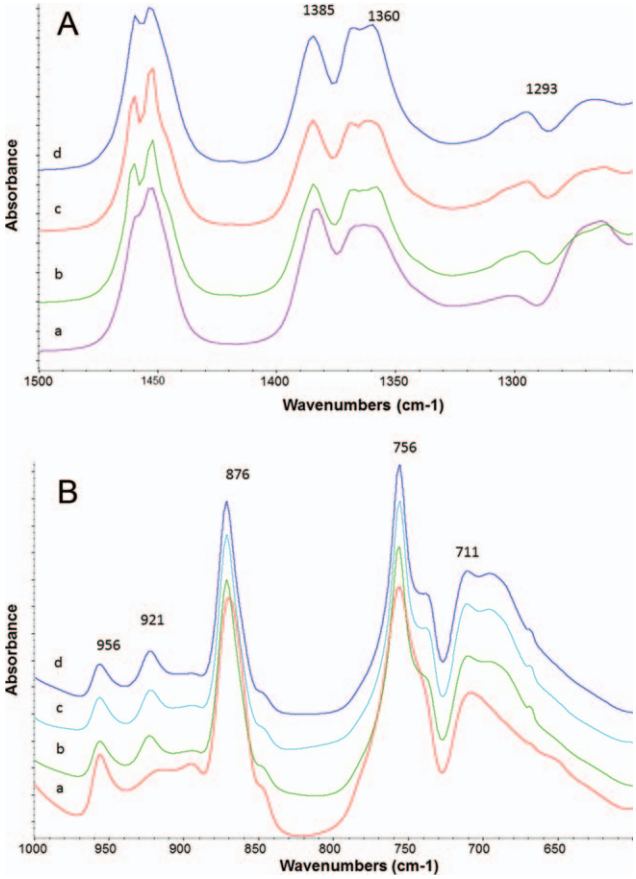

Figure 2. A: FTIR spectra of PLLA films at various annealing temperatures in the region of 1500–1200 cm^{-1}: (a) 25, (b) 80, (c) 95, and (d) 110°C. B: FTIR spectra of PLLA films at various annealing temperatures in the region of 1000–600 cm^{-1}: (a) 25, (b) 80, (c) 95, and (d) 110°C. [Color figure can be viewed in the online issue, which is available at wileyonlinelibrary.com.]

was assigned to the amorphous phase. These bands were assigned to the coupling of C—C backbone stretching with CH_3 rocking mode which is very sensitive to 10_3 helical chain conformation of the α-crystals. Figure 2 shows no band at 908 cm^{-1}, suggesting that there is no detectable level of β crystal form present in our annealed PLLA.[38]

Ly and Vasanthan[37] studied crystallization and hydrolytic degradation of PLLA using FTIR spectroscopy. The infrared bands at 921 and 956 cm^{-1}, assigned to the combination of C—C back bone stretching and CH_3 rocking, were chosen to monitor structural changes that occurred during crystallization at different annealing temperatures and hydrolytic degradation in alkaline media.[37] The absorbance ratio of 921 and 956 cm^{-1} (A_{921}/A_{956}) provided a very good correlation with crystallinity obtained by DSC, shown in Figure 3(a). In this study structural changes occur during annealing and enzymatic degradation was investigated by FTIR spectroscopy. For a quantitative assessment of the degree of crystallinity, absorbance ratio, A_{921}/A_{956} was calculated. The absorbance ratio (A_{921}/A_{956}) is plotted against T_a in Figure 3(b). The A_{921}/A_{956} absorbance ratio increases with increasing T_a, suggesting an increase in crystallinity of PLLA with T_a.

Applied Polymer SCIENCE

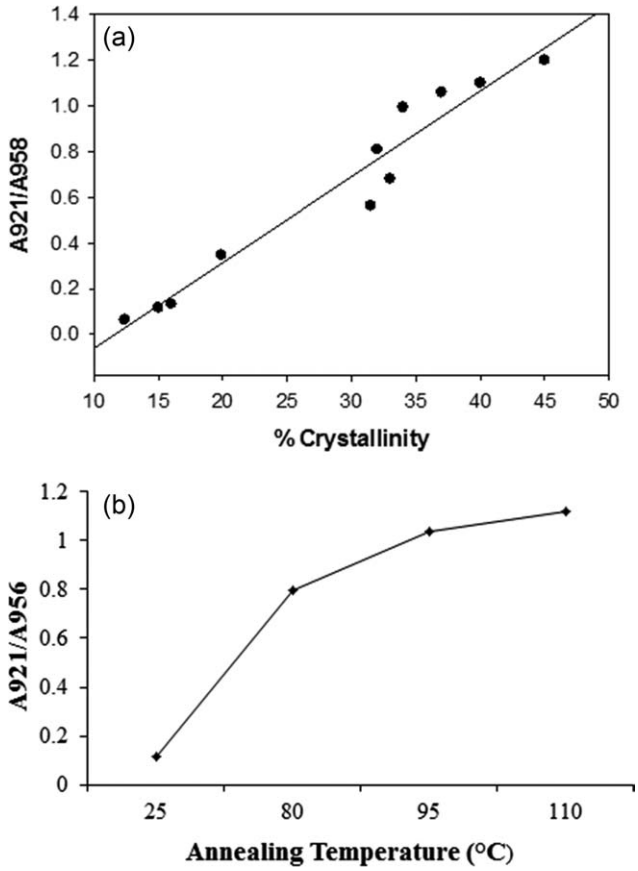

Figure 3. (a) Absorbance ratio (A_{921}/A_{956}) versus DSC crystallinity. (b) Absorbance ratio (A_{921}/A_{956}) versus annealing temperatures (T_a).

Enzymatic Degradation

Figure 4 shows the percentage of weight loss as a function of hydrolysis time. Weight loss of the annealed PLLA films is compared with neat PLLA film. It is clear from Figure 4 that the percentage of weight loss increases linearly with increasing degradation time. A control film was placed in water for 9 days at 37°C and no change in the mass was observed. This suggests no hydrolytic degradation during the time enzymatic hydrolysis was carried out. It appears that the highest weight loss was observed for the PLLA25 and the least weight loss was observed for PLLA110. The percentage of weight loss observed in 9 days for various PLLA films is given in Table I. Approximately 40% of weight loss occurred for PLLA25 after 9 days of enzymatic degradation and only 5.4% of weight loss was observed for the films annealed at PLLA110 during the same time period, indicating that the extent of degradation by enzyme decreases with increasing crystallinity. The rate of degradation can be qualitatively compared using the slope of the curve. It is apparent that the slope decreases with increasing crystallinity, suggesting that the rate of degradation decreases with increasing crystallinity of PLLA films, suggesting that enzyme preferentially attacks the amorphous or less ordered region more than the crystalline region.

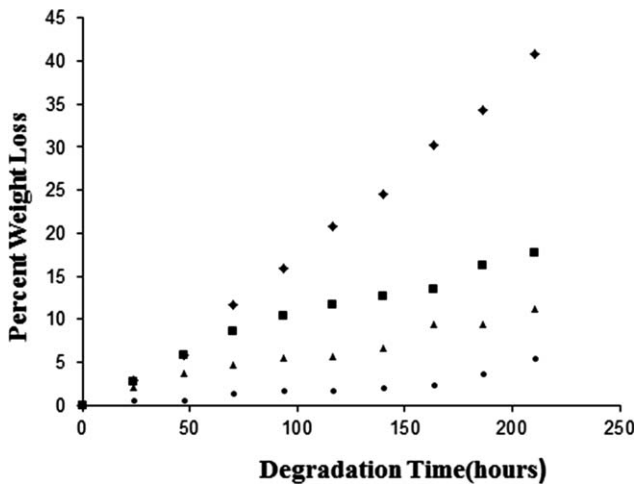

Figure 4. Percentage weight loss as a function of hydrolysis time for PLLA films annealed at different temperatures: (◆) PLLA25, (■) PLLA80, (▲) PLLA95, and (●) PLLA110.

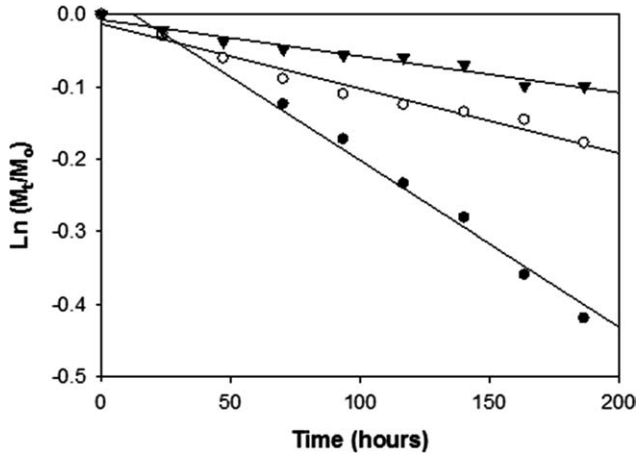

Figure 5. First-order reaction kinetics plots of the samples annealed at various temperatures: (●) PLLA25, (○) PLLA80, and (▲) PLLA95.

Base hydrolysis of PLLA in the presence of 0.1*M* NaOH was carried out[37] and it was found that the degradation increased with increasing crystallinity, suggesting that the degradation mechanism of enzymatic hydrolysis of PLLA is significantly different

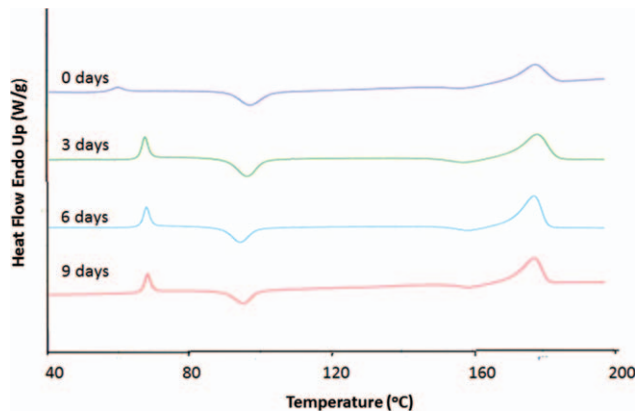

Figure 6. DSC scans of PLLA films as-cast film before and after hydrolysis for 3, 6, and 9 days. [Color figure can be viewed in the online issue, which is available at wileyonlinelibrary.com.]

Table II. Glass Transition, Cold Crystallization, and Melting Temperature of Annealed PLLA Films Before and After Enzymatic Degradation for 3, 6, and 9 Days

	Sample								
	PLLA25			PLLA80		PLLA95		PLLA110	
Degradation time (day)	T_g	T_c	T_m	T_g	T_m	T_g	T_m	T_g	T_m
0	59	89	170	61	170	-	170	-	170
3	65	90	171	65	172	65	171	66	172
6	66	88	172	65	171	67	171	67	172
9	68	92	173	67	170	65	170	67	172

from base hydrolysis of PLLA. On the other hand enzymatic degradation has been shown to decrease with increasing crystallinity.[30–35] Enzymatic hydrolysis of PLLA without free amorphous region was studied. It was demonstrated an increase in crystallinity with degradation time and concluded that degradation proceeds mainly at the restricted amorphous region.[30] In this study, the enzymatic degradation of PLLA25 showed an increase in crystallinity with degradation time whereas the enzymatic degradation of PLLA80, PLLA95, and PLLA-110 showed no significant change in crystallinity with time. Semicrystalline polymers generally consist of two components, the crystalline and the amorphous phase and two-component assumption was found to be generally valid for PLLA. Amorphous component can include restricted amorphous (chain fold, chain ends and inter lamellar traverses) and free amorphous phase. The degradation rate of restricted amorphous component is usually much slower compared to free amorphous component. It appears that degradation occurs in both free and restricted amorphous region in the as-cast film and crystallinity of degraded film increases with time due to degradation of restricted amorphous phase. The restricted amorphous phase gets smaller due to lamellar thickening during annealing and therefore degradation occurs predominantly in the free amorphous region that leads to no significant change in crystallinity with degradation time, confirmed by both DSC and FTIR spectroscopy.

Degradation kinetics was studied to understand the mechanism associated with enzymatic degradation. The degradation rate can be studied either the rate of formation of degradation products or rate of disappearance of PLLA at a given enzyme concentration. Since number average molecular (M_n) weight is directly related to the scission of polymer chain, it was used extensively to study degradation kinetics. This does not accurately predict the hydrolysis rate of the polymer. Hydrolysis reaction occurs between ester linkage and water and therefore it is reasonable to assume rate of degradation is directly proportional to the concentration of ester groups. The number of ester linkages is proportional to mass of the polymer and therefore degradation kinetics was analyzed using the initial and final masses, as well as the degradation times, to determine the order of the reaction. The kinetics of polymer degradation can be described by the following equation:

$$dM/dt = kM^n$$

$$\log\, dM/dt = \; n \log M + \log\, k,$$

where dM/dt represents the rate of degradation, M is the mass, k is the rate constant, and n is the order of reaction to be determined. Log dM/dt was plotted against log M and the order of the reaction was determined as first order. The integrated law of first-order equation can be written as:

$$\ln M_t/M_o = -kt$$

where M_t/M_o is the relative weight remaining at a given time, k is the first-order rate constant, and t is the time. Plots of ln M_t/M_o versus t are shown for PLLA-25, PLLA-80, and PLLA-95 in Figure 5. PLLA-110 degraded only about 5% and therefore it is not included in Figure 5. All of them showed a correlation between 0.90 and 0.99. Degradation rate constants were determined from the slope and the half-life ($t_{½}$) was determined from 0.693/k. The degradation rate constant, k and $t_{½}$, are given in Table I. It is apparent from Table I that the $t_{½}$ increases and k decreases with increasing crystallinity, indicating that the initial crystallinity of the PLLA film significantly affects the degradation rate and the extent of degradation. It should be pointed out that degradation kinetics was also analyzed using zero and second order kinetics. Our fitting shows degradation kinetics is better represented by first-order kinetics.

Morphological Changes of PLLA After Degradation

DSC heating scans of PLLA25, PLLA80, PLLA95, and PLLA110 before and after 3, 6, and 9 days of degradation and DSC scan of PLLA25 before and after 3, 6, and 9 days of degradation is shown

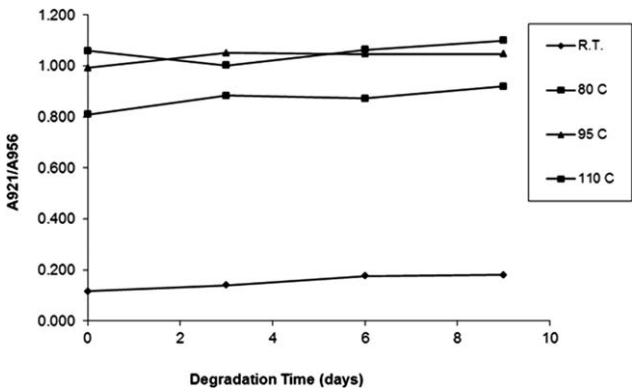

Figure 7. Plot of absorbance ratio (peak area) of crystalline and amorphous bands (A_{921}/A_{956}) versus degradation time for the films annealed at 25, 80, 95, and 110°C.

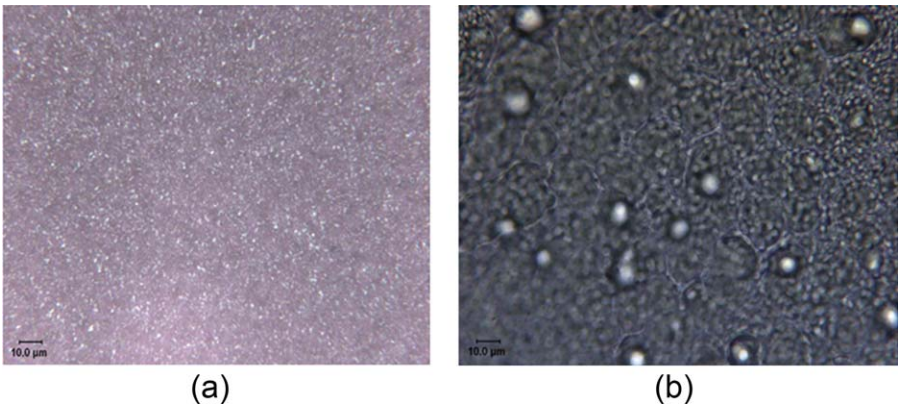

Figure 8. Optical micrograph of PLLA film: (a) PLLA80 before degradation and b) PLLA80, degraded for 6 days. [Color figure can be viewed in the online issue, which is available at wileyonlinelibrary.com.]

in Figure 6. The T_g, T_c, and T_m values are shown in Table II. It can be seen from Table II that the T_g, T_c, and T_m values for as-cast PLLA film show an increase after 3 days of degradation, but no significant change was detected for the films degraded for more than 3 days. The values stayed almost constant for the films degraded for 6 and 9 days. The T_g was not detected for PLLA films annealed at different temperatures before degradation. As the thermally induced crystallization occurs, the mobility of polymer chains in the amorphous phase might be reduced, leading the T_g to increase and disappear after certain T_a. The T_g is apparent in all of the degraded films and is shifted to a higher temperature with increasing degradation time. A control experiment was carried by immersing as-cast PLLA film for 10 days and shown no change in T_g with time. This observation ruled out the water absorption is responsible for reappearance of T_g. Therefore reappearance of T_g may be explained by enthalpy of relaxation. The reduction of free volume occurs due to aging that increases the T_g. Melting temperatures were compared before and after degradation of PLLA and it can be seen that T_m values do not change significantly during the degradation process for all of the annealed films, suggesting that crystalline region was not hydrolyzed. On the other hand, melting temperature of as-cast PLLA film increases with degradation time, again conformed hydrolyzes of restricted amorphous phase.

The change in crystallinity during the enzymatic degradation was analyzed using DSC. It was found that crystallinity of as-cast PLLA films increased from 17 to 32% after 10 days of degradation; whereas crystallinity of all annealed films showed no significant change up to 10 days of degradation. Crystallinity changes were also monitored using absorbance ratio, A_{921}/A_{956} of IR bands at 921 and 956 cm^{-1} before and after degradation. Absorbance at 921 and 956 cm^{-1} were attributed previously to the crystalline phase and the amorphous phase, respectively. Figure 7 shows the A_{921}/A_{956} versus degradation time. It can be seen in Figure 7 that the absorbance ratio A_{921}/A_{956} showed an increase for as-cast PLLA films and no significant change with increasing degradation time for all annealed films, in agreement with our DSC results. An increase in crystallinity obtained by both DSC and FTIR methods for as-cast PLLA film is attributed to degradation of restricted amorphous phase.

PLLA films were examined using optical light microscopy before and after degradation to observe the morphological changes. Two different optical microscopic techniques were used; polarizing microscopy without analyzer and polarizing microscopy with analyzer. PLLA films that annealed at 80 and 110°C before and after 6 days of degradation were chosen for the analysis with the optical microscope. Figure 8(a) shows the appearance of the 80°C annealed PLLA film before degradation. The film

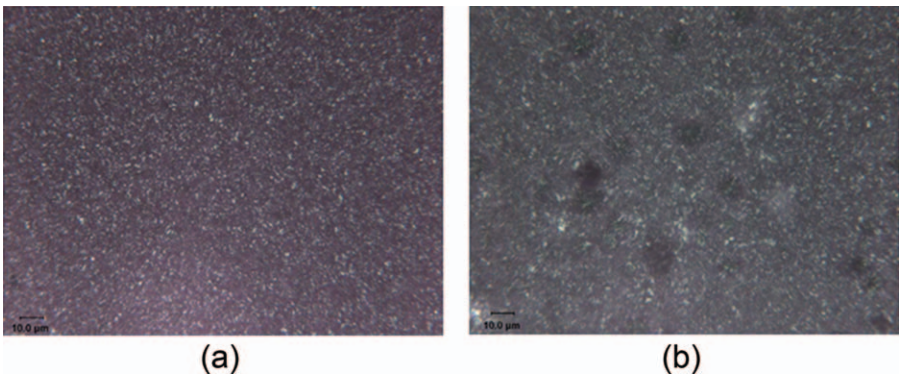

Figure 9. Optical micrograph of PLLA film PLLA110 before degradation and b) PLLA110, degraded for 6 days. [Color figure can be viewed in the online issue, which is available at wileyonlinelibrary.com.]

appeared birefringent having regular distribution of small spherulites. Figure 8(b) illustrates the features observed in the sample 80°C annealed PLLA sample after 6 days of degradation. Spherulites and regular distribution of pores are apparent in the micrograph, suggesting that significant amount of enzymatic degradation occurs after 6 days. The optical micrograph was observed with the analyzer removed. Phase or domain boundaries were clearly apparent and are not shown here. Figure 9(a) illustrates the appearance of the 110°C annealed PLLA film before degradation. The film appeared birefringent having regular distribution of spherulites. Figure 9(b) displays the features observed for PLLA film annealed at 110°C after 6 days of degradation and a small number of pores are seen in Figure 10(b). Some regions appeared to have less degradation than others but overall they showed apparently less degradation than the 80°C annealed film, which is consistent with our weight loss study.

CONCLUSIONS

The effect of thermally induced crystallization by annealing on the enzymatic degradation of PLLA was investigated by weight loss, DSC, optical microscopy, and FTIR spectroscopy. PLLA films prepared by solvent casting method were annealed at different temperatures and structural changes were studied using DSC and FTIR spectroscopy. Three transitions (T_g, T_c, and T_m) were detected for the solvent cast films. PLLA films annealed at 80°C showed two transitions (T_g and T_m) and films annealed at higher temperatures showed only melting transition. The percent of crystallinity obtained by DSC, as well as FTIR spectroscopy, showed an increase with increasing T_a. The enzymatic degradation of PLLA was examined and compared with base hydrolysis of PLLA. The percentage of weight loss and degradation kinetics was found to depend on initial crystallinity of the PLLA film. The highest weight loss was obtained for low crystalline samples and suggested that degradation occurs preferentially in the free amorphous phase. Enzymatic degradation kinetics was found to follow the first-order kinetics. Rate constants decreased and half-time of degradation increased with increasing crystallinity. The T_g, T_c, and T_m values stayed almost constant after 3 days of degradation. Crystallinity of degraded films was obtained by DSC and IR spectroscopy and showed no significant change with increasing degradation time. It has been concluded that degradation occurs predominantly in the free amorphous region of annealed PLLA films.

ACKNOWLEDGMENTS

This work has been partially supported by Department of Commerce and National Textile Center. The authors thank NSF for providing funds for the purchase of a GC–MS (CHE-0840432). The authors also thank reviewers for their helpful suggestions to improve the quality of this article.

REFERENCES

1. Auras, R.; Harte, B.; Selke, S. *Macromol. Biosci.* **2004,** *4*, 835.
2. Garlotta, D. J. *Polym. Environ.* **2001,** *9*, 63.
3. Jain, R. J. *Biomaterials* **2000,** *21*, 2475.
4. Lee, J. H.; Park, T. G.; Park, H. S.; Lee, D. S.; Lee, Y. K.; Yoon, S. C.; Nam, J. D. *Biomaterials* **2003,** *24*, 2773.
5. Nam, Y. S.; Park, T. G. *Biomaterials* **1999,** *20*, 1783.
6. Grijpma, D. W.; Pennings, A. J. *Macromol. Chem. Phys.* **1994,** *195*, 1633.
7. Okuzaki, H.; Kubota, I.; Kunugi, T. J. *Polym. Sci, Phys.* **1999,** *37*, 991.
8. Kulkarni, R. K.; Moore, E. G.; Hegyeli, A. F.; Leonard, F. J. *Biomed. Mater. Res* **1971,** *5*, 169.
9. Zhang, J.; Tsuji, H.; Noda, I.; Ozaki, Y. J. *Phys. Chem. B* **2004,** *108*, 11514.
10. Iwata, T.; Doi, Y. *Macromolecules* **1998,** *31*, 2461.
11. Fujita, M.; Doi, Y. *Biomacromolecules* **2003,** *4*, 1301.
12. Di Lorenzo, M. L. *Eur. Polym. J.* **2005,** *41*, 569.
13. Li, S.; McCarthy, S. *Biomaterials* **1999,** *20*, 35.
14. Tsuji, H.; Ikada, Y. *Polymer* **1995,** *36*, 2709.
15. Yasuniwa, M.; Iura, K.; Dan, Y. *Polymer* **2007,** *48*, 5398.
16. Vasanthakumari, R.; Pennings, A. J. *Polymer* **1983,** *24*, 175.
17. Kalb, B.; Pennings, A. J. *Polymer* **1980,** *21*, 607.
18. Baratian, S.; Hall, E. S.; Lin, J. S.; Xu, R.; Runt, J. *Macromolecules* **2001,** *34*, 4857.
19. DeSantis, P.; Kovacs, A. J. *Biopolymers* **1968,** *6*, 299.
20. Kolstad, J. J. *J. Appl. Polym. Sci.* **1996,** *62*, 1079.
21. Hoogsteen, W.; Postema, A. R.; Pennings, A, J.; ten Brinke, G.; Zugenmaier, P. *Macromolecules* **1990,** *23*, 634.
22. Li, S.; Vert, M. In Degradable Polymers, Principle; Applications; Chapman & Hall: London, **1995.**
23. Albertsson, A. C., Ed. Degradable Aliphatic Polyesters: Advances in Polymer Science, Vol. *157*. Springer: Berlin, Germany, **2002.**
24. Weir, N. A.; Buchanan, F. J.; Orr, J. F.; Farrar, D. F.; Boyol, A. *Biomaterials* **2004,** *25*, 3939.
25. Ikada, Y.; Tsuji, H. *Macromol. Rapid Commun.* **2000,** *21*, 117.
26. Scott, G. *Macromol. Symp.* **1999,** *144*, 113.
27. Schnabel, W. Polymer Degradation-Principles and Practical Applications. USA: Oxford University Press, **1988.**
28. Tsuji, H.; Tezuka, Y.; Yamada, K. J. *Polym. Sci. Part B: Polym. Phys.* **2005,** *43*, 1064.
29. Innance, S.; Maffezzoli, A.; Leo, G.; Nicolais, L. *Polymer* **2001,** *42*, 3799.
30. Tsuji, H.; Ishizaka, T. *Macromol. Biosci.* **2001,** *1*, 59.
31. Crescenzi, V.; Manzini, G.; Calzolari, G.; Borri, C. *Eur. Polym. J.* **1972,** *8*, 449.
32. Tsuji, H.; Ikarashi, K. *Polym. Degrad. Stab.* **2004,** *85*, 647.
33. Tsuji, H.; Nakahara, K. J. *Appl. Polym. Sci.* **2002,** *86*, 186.
34. Tsuji, H.; Suzuyoshi, K. *Polym. Degrad. Stab.* **2002,** *75*, 357.
35. Cam, D.; Hyon, S.-H.; Ikada, Y. *Biomaterials* **1995,** *16*, 833.
36. Tsuji, H.; Ikada, Y. *Polym. Degrad. Stab.* **2000,** *67*, 179.
37. Vasanthan, N.; Ly, O. *Polym. Degrad. Stab.* **2009,** *94*, 1364.
38. Zhang, J. M.; Duan, Y.; Sato, H.; Tsuji, H.; Noda, I.; Yan, S.; Ozaki, Y. *Macromolecules* **2005,** *38*, 8012.
39. Zhang, J. M.; Tsuji, H.; Noda, I.; Ozaki, Y. *Macromolecules* **2004,** *37*, 6433.